Pergamon

Acta mater. Vol. 46, No. 10, pp. 3399–3408, 1998

Printed in Great Britain
PII: S1359-6454(98)00049-4
1359-6454/98 $19.00 + 0.00

ISOTHERMAL CREEP OF METALLIC GLASSES: A NEW APPROACH AND ITS EXPERIMENTAL VERIFICATION

V. A. KHONIK[1]†, A. T. KOSILOV[2], V. A. MIKHAILOV[1] and V. V. SVIRIDOV[1]

[1]Department of General Physics, State Pedagogical University, Lenin Street 86, 394043 Voronezh and [2]Department of Metal Physics, State Technical University, Moskovsky Avenue 14, 394028 Voronezh, Russia

(Received 24 March 1997; accepted 5 February 1998)

Abstract—An extended version of the theory of structural relaxation in metallic glasses under the action of external stress is presented. The theory explains the structural relaxation as a set of irreversible noncorrelated two-stage elementary shear atomic rearrangements with continuously distributed activation parameters in distinct regions of structure—relaxation centres. In loaded samples structural relaxation results in an accumulation of plastic deformation in accordance with magnitude and orientation of the applied stress. General equations are obtained for the creep strain rate as a result of the irreversible directed structural relaxation. Specially designed experiments were performed to test the theory. It is shown that the theory gives an adequate interpretation of experimental creep kinetics except for the time interval that covers 10^1–10^2 s after loading. This initial creep stage is supposed to result from reversible atomic rearrangements in relaxation centres with a symmetrical two-well potential. © *1998 Acta Metallurgica Inc.*

1. INTRODUCTION

Metallic glasses (MGs) are highly nonequilibrium structures. This fact is the origin of spontaneous internal atomic rearrangements which lead to changes of all physical properties and are known generally as "structural relaxation" (SR). Probably it is an accumulation of inelastic deformation which is influenced the strongest by SR. For example, the Newtonian viscosity of MGs is known to increase by up to five orders of magnitude owing to SR [1]. Such a strong influence of SR on atomic mobility requires a primary explanation. However, no decisive progress in this field has yet been achieved despite twenty-year-long investigations.

Attempts to formulate a quantitative model of SR under external load have been started with the so-called free volume models of Spaepen [2] and Argon [3], which have very similar physical foundations. The former model was subsequently improved in several directions [4–7]. In summary, the "free volume model" [2, 4–7] assumes that inelastic flow is provided by some "flow defects" which can annihilate at some special places of structure—"relaxation sites". It was implied also, in fact (i.e. in the flow equations), that the plastic deformation is characterized by a single activation energy.

A. van den Beukel and coworkers, in a series of papers [8–16], have proposed another way to describe the SR. They considered two relaxation components: the first component due to the compositional short-range ordering (CSRO) and the second one determined by the topological ordering (TSRO). These components were assumed to be time separated allowing their individual identification. An extended spectrum of activation energies is an inherent feature of CSRO in this approach. Therefore, CSRO could be described in terms of the activation energy spectrum model. The main equations of this model were obtained by Primak as early as 1955 [17] and applied later by Argon, and Gibbs *et al.* [18–21] to relaxation phenomena in glasses. The CSRO is followed by the topological ordering which can be described by the free volume model with a single activation energy. The considerations of van den Beukel were criticized [21] for an obvious reason: any rearrangement of chemically different atoms cannot be realized without some changes in structure topology. So, any time separation of these two components of the relaxation process does not seem to be physically based. Therefore, the author pointed out himself (see, e.g. Refs [12, 13]) that there arose several difficult questions when the concept is compared with the experiment in detail.

In the present authors' opinion, any attempt of adequate interpretation of all the SR kinetics features under external stress must address the continuous activation energy spectrum of atomic rearrangements. A wide distribution of microscopic quantities which control processes of different nature is the most distinctive feature of glasses and identifying them as the opposite to crystals. Numerous investigations of the past decade have demonstrated quite convincingly this notion to be

†To whom all correspondence should be addressed.

indispensable, in particular when analyzing the inelastic flow under conditions of intensive SR [21–29]. However, a serious attempt to take the SR spectrum into account was realized only by Knuyt *et al.* [30].

If one considers the simplest case of the SR under stress, namely creep, then there are three important experimental facts which have to be explained: (i) the linear increase of the Newtonian viscosity with time under isothermal testing [3–5, 31]; (ii) the strong influence of the specimen's thermal prehistory on the relaxation kinetics [1]; and (ii) the Newtonian flow at low stresses and transition to a nonlinear deformation on applied load increase [32].

The above-mentioned theoretical models have not reached any essential success in quantitative interpretation of all these experimental facts *simultaneously*. A new concept of SR under external stress was presented [33, 34] which has made possible a quantitative interpretation of MG creep laws. This concept has been further refined and applied to an analysis of some other SR-induced mechanical relaxation phenomena (creep, stress relaxation, active loading and low-frequency internal friction under isothermal or linear heating conditions) [35–45]. Here we present a generalized form of the concept [33–45] as applied to isothermal creep together with results of a specially designed experiment.

2. THE CONCEPT OF THE DIRECTED STRUCTURAL RELAXATION

We consider structural relaxation of MGs to be a consequence of (i) spatially separated, (ii) noncorrelated, and (iii) irreversible (for the most part) elementary atomic shear rearrangements with distributed activation energies. These processes occur in particular regions of the structure, called relaxation centers, RCs (Fig. 1). Each rearrangement is considered to be a two-stage process. In stage I a thermally activated shear event is realized in some volume V_0 (to be of the order of the first coordination sphere volume) occupied by the atoms which directly contribute to the work of external forces to overcome the activation barrier. Orientation of this shear (see pair arrows in Fig. 1) is defined by the exact atomic configuration in the volume V_0 and is independent of applied stress orientation. The orientation of external stress, however, influences the activation barrier of the shear. Atomic configurations under discussion can be considered as "retainers" [33, 34] which hold back plastic deformation in nearby regions of the material. Thermally activated removal of a retainer leads immediately to cooperative displacements of atoms in the nearest environment. This process results in viscous flow in some volume Ω (Fig. 1) comprising the volume V_0 and is interpreted as the stage II of an elementary shear relaxation event.

Atomic displacements in the volume Ω result in plastic deformation which consists of a hydrostatic compression and a shear of random (in the absence of external stress) orientation. Averaging of such shears over different Ω gives no macroscopic deformation. External stress induces anisotropy of the elementary shears selecting some of their directions to be realized with a greater probability. This results in accumulation of macroscopic plastic deformation in strict accordance with orientation and magnitude of external load. There arises a "directed

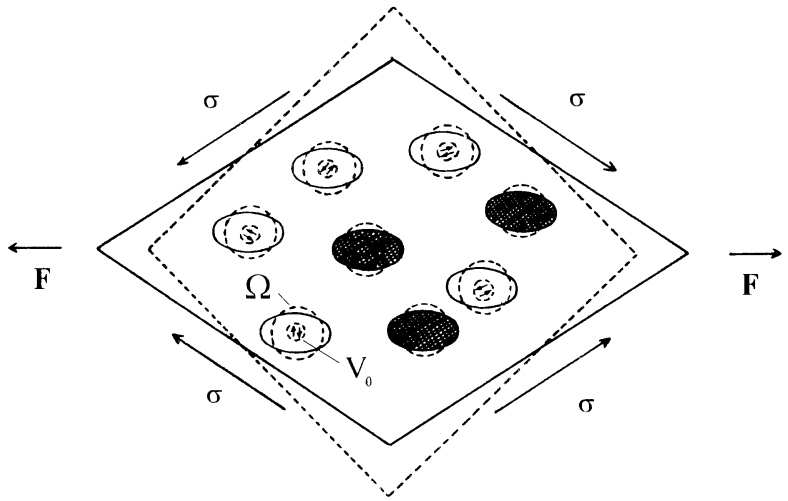

Fig. 1. A schematic drawing of MG structural relaxation under external stress as a set of irreversible atomic rearrangements in relaxation centers. Paired arrows inside small circles indicate directions of possible shears at stage I of elementary relaxation events. Larger circles correspond to material to be transformed at stage II. Dashed (solid) circles and lines denote MG before (after) loading. Shaded ellipses show transformed relaxation centers. Volumes V_0 and Ω of stages I and II of an elementary shear are indicated.

structural relaxation", i.e. the stress-oriented structural relaxation.

3. ACTIVATION PARAMETERS OF RELAXATION CENTRES

During a transformation into the low-energy configuration under stress σ_{ij} at a temperature T, an activation barrier $\Delta G(\sigma_{ij},T)$ has to be overcome, which is the difference in the Gibbs potential between the saddle-point and the metastable configurations of the RC. Expanding ΔG in a Taylor series in terms of σ_{ij} gives

$$\Delta G \approx E - \sigma_{ij} V_{ij} \tag{1}$$

where E is the stress-independent part of ΔG (the "activation energy"), V_{ij} the tensor of activation volumes, which characterizes the work of the stress to activate an RC. In accordance with the concept formulated in the previous section, the activated state is achieved by shearing in some definite plane along a certain direction. If one denotes the unit vector normal to the shear plane as **n** and the unit vector in the shear direction as **s**, then the simplest form of the activation volume tensor is

$$V_{ij} = V\left(n_i s_j + n_j s_i\right) \tag{2}$$

where $V>0$ is a scalar random value being determined by the RC atomic configurations. Orientations of **n** and **s** are implied random as well.

The normal **n** to the shear plane is determined by the polar angle θ and the axial angle φ relative to some Cartesian coordinate axes (Fig. 2):

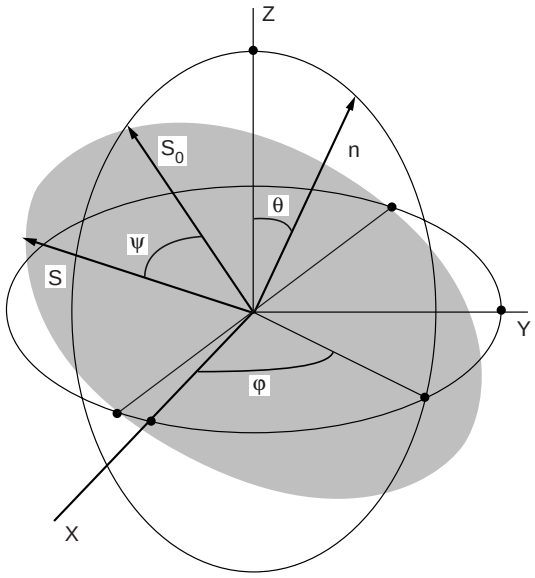

Fig. 2. Orientation of an elementary shear system. The shear plane is shaded. Radii of all the circles are 1. The equatorial plane and the meridional plane containing vectors **n** and **s** are shown by thin lines. Directional angles θ' and φ' of the shear vector **s** are not shown.

$$\mathbf{n} = (\sin\theta\cos\varphi,\ \sin\theta\sin\varphi,\ \cos\theta). \tag{3}$$

Only the values $\theta \in [0, \pi/2]$ are of physical meaning. Any set $\{\theta,\varphi\}$ with $\theta > \pi/2$ is equivalent to the set $\{\pi - \theta, \varphi \pm \pi\}$. The orientation of **s** is more conveniently defined by the angle ψ counted in the shear plane from the unit vector $\mathbf{s_0} = (-\cos\theta\cos\varphi,\ -\cos\theta\sin\varphi,\ \sin\theta)$, which lies in the intersection of the shear plane and the meridional plane containing **n** (Fig. 2):

$$\left.\begin{aligned} \mathbf{s_0 n} &= 0, \\ \mathbf{e_z}(\mathbf{n} \times \mathbf{s_0}) &= 0, \end{aligned}\right\} \ -\ \text{definition of } \mathbf{s_0} \tag{4a}$$

$$\mathbf{s} = (\sin\theta'\cos\varphi',\ \sin\theta'\sin\varphi',\ \cos\theta')\ -\ \text{definifion of } \mathbf{s} \tag{4b}$$

$$\mathbf{s_0 s} = -\cos\theta\sin\theta'\cos(\varphi - \varphi') + \sin\theta\cos\theta'$$

$$= \cos\psi\ -\ \text{definitionof } \psi. \tag{4c}$$

Considering the orientation of an RC shear system not correlated with the activation volume and energy of RC, **n** and **s** to be distributed uniformly over the hemisphere of $0 \le \theta \le \pi/2$, $0 \le \varphi \le 2\pi$ and the circumference of $0 \le \psi < 2\pi$, respectively, one may put down the spectrum of activation parameters in the as-quenched state as

$$\mathrm{d}N_0(E, V, \theta, \varphi\ \psi)$$

$$= N_0 w(E, V)\mathrm{d}E\mathrm{d}V \frac{1}{4\pi^2} \sin\theta\ \mathrm{d}\theta\ \mathrm{d}\varphi\ \mathrm{d}\psi \tag{5}$$

where N_0 is the mean number of RCs per unit volume of as-quenched MG, $\mathrm{d}N_0(E, V, \theta, \varphi, \psi)$ the number of RCs with activation energies of E to $E + \mathrm{d}E$, scalar activation volumes of V to $V + \mathrm{d}V$ and orientation (θ,φ,ψ). $w(E, V)$ is the joint distribution density of random E and V values normalized as

$$\int_0^\infty \int_0^\infty w(E,V)\mathrm{d}E\mathrm{d}V = 1.$$

4. KINETICS OF PREANNEALING

It was shown earlier [33, 34, 37] that to describe correctly the SR under external stress one has to take into consideration a preliminary exposure time τ of as-quenched sample *without* load when RCs work out spontaneously, being driven by thermal fluctuations. Let the probability for an RC to work out be dependent only on its activation energy at this preannealing stage. Then the delay law for the number of remaining RCs is

$$\frac{\mathrm{d}}{\mathrm{d}t}\mathrm{d}N(E, V, \theta, \varphi, \psi, \tau) = -\nu \mathrm{e}^{-\frac{E}{kT_0}}\mathrm{d}N(E, V, \theta, \varphi, \psi, \tau) \tag{6}$$

where ν is the characteristic frequency being of the order of the Debye frequency, and T_0 is the preannealing temperature. Integrating equation (6) gives the distribution of activation parameters of RCs at the end of the preannealing:

$$\mathrm{d}N(E, V, \theta, \varphi, \psi, \tau) = dN_0(E, V, \theta, \varphi, \psi)F\left(\nu\tau, \frac{E}{kT}\right) \tag{7}$$

where the cutting function

$$F(\alpha,\beta E) = \exp\left(-\alpha \mathrm{e}^{-\beta E}\right). \tag{8}$$

Local relaxation at stage I without external load is directed by internal stresses. Since these are isotropic on average, the activation events of the RCs result in no macroscopic deformation. Thus, the main effect of preannealing consists in cutting off the low-energy tail in the initial distribution of activation parameters as described by the factor F in equation (7). The cutting function $F(E)$ looks roughly like a unit step at the characteristic energy $E_0 = \beta^{-1}\ln\alpha$. The derivative $\mathrm{d}F/\mathrm{d}E$ has a narrow width maximum of about $2.5/\beta$. For calculations it is convenient to use the fact that $\lim_{\beta\to\infty} \mathrm{d}F/\mathrm{d}E = \delta(E - E_0)$. It means that if the scale of significant changes in some fluncion $g(E)$ is greater than the thermal energy $kT = \beta^{-1}$, then

$$\int_0^\infty g(E)\frac{\mathrm{d}F}{\mathrm{d}E}\mathrm{d}E \approx g(E_0) = g\left(\beta^{-1}\ln a\right). \tag{9}$$

Note that the usage of equation (9) is practically equivalent to the straightforward "step approximation" [33, 34, 37] but is more convenient mathematically.

5. GENERAL RELATIONS FOR ISOTHERMAL CREEP

Let a sample be loaded by the uniaxial stress along the z axis:

$$\sigma_{ij} = \sigma\delta_{i3}\delta_{j3}. \tag{10}$$

Then the activation barrier for an RC with given values of activation parameters E, V, θ, φ, ψ is:

$$\Delta G = E - \sigma_{33}V_{33} = E - \sigma\gamma V \tag{11}$$

where

$$\gamma = 2n_3 s_3 = 2\cos\theta\cos\theta' = \sin 2\theta\cos\psi \tag{12}$$

is the orientational factor. Here we have used the perpendicularity of the vector **s** to **n** and equation (4c) to calculate the polar angle θ' of the shear vector **s**.

Under uniaxial external stress the structural relaxation becomes anisotropic as well, as was discussed in the Section 2. Neglecting the volume shrinkage, one may write the resulting macroscopic shear deformation as

$$\varepsilon(t) = u_0\Omega\left(N_\tau - \int \mathrm{d}N(E,V,\theta,\varphi,\psi,t)\right) \tag{13}$$

where $N_\tau = \int \mathrm{d}N(E,V,\theta,\varphi,\psi,\tau)$ is the overall number (per unit volume) of RCs that survived preannealing, and u_0 is the mean plastic deformation resulting from an elementary shear event. It was estimated earlier that $u_0 = C\sigma$, where C is some constant [35, 37].

The time dependence of the distribution of RCs, $\mathrm{d}N$, is defined by the delay law similar to equation (6), but accounting for stress-induced changes in activation barriers:

$$\frac{\mathrm{d}}{\mathrm{d}t}\mathrm{d}N(E,V,\theta,\varphi,\psi,t) = -\nu \mathrm{e}^{-\frac{(E-\gamma(\theta,\psi)\sigma V)}{kT}}\mathrm{d}N(E,V,\theta,\varphi,\psi,t) \tag{14}$$

where T is the creep testing temperature which may not generally be equal to the preannealing temperature T_0. Integrating this equation yields

$$\mathrm{d}N = \frac{N_0}{4\pi^2}\mathrm{d}E\mathrm{d}V\sin\theta\mathrm{d}\theta\mathrm{d}\varphi\mathrm{d}\psi w(E,V) \underbrace{\times\exp\left(-\nu\tau \mathrm{e}^{-\frac{E}{kT_0}}\right)}_{F\left(\nu\tau, \frac{E}{kT_0}\right)} \underbrace{\exp\left(-\nu t \mathrm{e}^{\frac{\gamma\sigma V}{kT_e}}\mathrm{e}^{-\frac{E}{kT}}\right)}_{F\left(\nu t \mathrm{e}^{\frac{\gamma\sigma V}{kT}}, \frac{E}{kT}\right)}. \tag{15}$$

We used here equations (5), (7), and (8) and restarted the count-time t from the end of preannealing.

Calculations will be greatly simplified without a loss of physical meaning if we consider a particular case when both creep testing and preannealing are carried out at the same temperature, i.e. at $T = T_0$. This allows reduction of the products of cutting functions describing preannealing and annealing under stress to a single cutting function. For example, in equation (15)

$$F\left(\nu\tau, \frac{E}{kT_0}\right)F\left(\nu t \mathrm{e}^{\frac{\gamma\sigma V}{kT}}, \frac{E}{kT}\right)\Bigg|_{T=T_0} = F\left(\nu\left(\tau + t\mathrm{e}^{\frac{\gamma\sigma V}{kT}}\right), \frac{E}{kT}\right). \tag{16}$$

Other useful simplifications are based on the identity

$$\frac{\partial}{\partial t}F\left(\nu t, \frac{E}{kT}\right) \equiv -\frac{kT}{t}\frac{\partial}{\partial E}F\left(\nu t, \frac{E}{kT}\right) \tag{17}$$

which follows immediately from the definition of

the cutting function F. The main quantity of interest is the creep strain rate $\dot{\varepsilon} = \mathrm{d}\varepsilon/\mathrm{d}t$. Using equations (13), (15) and (17) it can be written as

$$\dot{\varepsilon} = \frac{C\Omega N_0 kT}{2\pi}\sigma\int_0^{\pi/2}\sin\theta\mathrm{d}\theta\int_0^{2\pi}\mathrm{d}\psi\int_0^{\infty}\frac{\mathrm{d}V}{t+\tau_{\mathrm{eff}}(\gamma V)}\int_0^{\infty}$$

$$\times\mathrm{d}E w(E,V)\frac{\partial}{\partial E}F\left(\nu\left(\tau + t\mathrm{e}^{\frac{\gamma\sigma V}{kT}}\right),\frac{E}{kT}\right) \qquad (18)$$

where

$$\tau_{\mathrm{eff}}(\gamma V) = \tau\mathrm{e}^{-\frac{\gamma\sigma V}{kT}}. \qquad (19)$$

As a rule, the thermal energy kT is small compared with the characteristic scale of the original spectrum $w(E,V)$ considered as a function of E. Then one may certainly suppose that the conditions of equation (9) are satisfied and use this relation to carry out integration over E in equation (18):

$$\dot{\varepsilon} = \frac{C\Omega N_0 kT}{\pi}\sigma\int_0^{\pi/2}\sin\theta\mathrm{d}\theta\int_0^{\pi}\mathrm{d}\psi\int_0^{\infty}\frac{\mathrm{d}V}{t+\tau_{\mathrm{eff}}(\gamma V)}$$

$$\times w\big(kT\ln\big[\nu\big(t+\tau_{\mathrm{eff}}(\gamma V)\big)\big]+\sigma\gamma V,V\big). \qquad (20)$$

We used also the fact that the expression under the integrals in equation (18) depends on ψ via the factor $\gamma\sim\cos\psi$, i.e. the contribution from the values of $\psi\in[\pi,2\pi]$ is the same as that from $\psi\in[0,\pi]$. Equation (20) can be rewritten in a more symmetric form by changing $\gamma V\to V$, and (for $\psi>\pi/2$) $\psi\to\pi-\psi$:

$$\dot{\varepsilon} = \frac{C\Omega N_0 kT}{\pi}\sigma\int_{-\infty}^{\infty}\frac{\mathrm{d}V}{t+\tau_{\mathrm{eff}}(V)}\int_0^{\pi/2}\frac{\mathrm{d}\theta}{\cos\theta}\int_0^{\pi/2}\frac{\mathrm{d}\psi}{\cos\psi}$$

$$\times w\left(kT\ln\big[\nu\big(t+\tau_{\mathrm{eff}}(V)\big)\big]+\sigma V,\frac{|V|}{\sin2\theta\cos\psi}\right). \qquad (21)$$

This is the main equation of the theory. It allows clarification of how the initial spectrum $w(E,V)$ influences the creep kinetics and to what degree the spectrum can be recovered from the observed kinetics.

6. A MODEL OF UNCOUPLING CORRELATION OF THE ACTIVATION PARAMETERS

The simplest assumption about the initial spectrum of activation parameters is

$$w(E,V) = \rho_{\mathrm{E}}(E)\rho_{\mathrm{V}}(V) \qquad (22)$$

where $\rho_{\mathrm{E}}(E)$ and $\rho_{\mathrm{V}}(V)$ satisfy the conditions

$$\int_0^{\infty}\rho_{\mathrm{E}}(E)\mathrm{d}E = 1$$

and

$$\int_0^{\infty}\rho_{\mathrm{V}}(V)\mathrm{d}V = 1.$$

Equation (22) implies that the activation energy of an RC does not correlate with the RC activation volume. Without considering the microscopic structure of RCs there are no essential reasons to prefer strongly this hypothesis to the opposite one. Should any information about the real distribution $w(E,V)$ be accessible, it could be treated in a way analogous to that sketched below.

Under the assumption given by equation (22) the main equation (21) takes the form

$$\dot{\varepsilon} = C\Omega N_0 kT\sigma\int_{-\infty}^{\infty}\frac{\rho_{\mathrm{E}}(E_0(V,t))}{t+\tau_{\mathrm{eff}}(V)}\mu(V)\mathrm{d}V \qquad (23)$$

where

$$E_0(V,t) = kT\ln\big[\nu\big(t+\tau_{\mathrm{eff}}(V)\big)\big]+\sigma V \qquad (24)$$

and

$$\mu(V) = \frac{1}{\pi}\int_0^{\pi/2}\frac{\mathrm{d}\theta}{\cos\theta}\int_0^{\pi/2}\frac{\mathrm{d}\psi}{\cos\psi}\rho_{\mathrm{V}}\left(\frac{|V|}{\sin2\theta\cos\psi}\right) \qquad (25)$$

is *orientation-averaged* distribution of activation volumes.

To calculate the angle integrals in equation (25) ρ_{V} is represented as

$$\rho_{\mathrm{V}}(V) = \int_0^{\infty}\rho_{\mathrm{V}}(V')\delta(V-V')\mathrm{d}V'. \qquad (26)$$

Substituting $\rho_{\mathrm{V}}(V)$ into equation (25) permits the integration over both θ and ψ and gives

$$\mu(V) = \int_{|V|}^{\infty}\rho_{\mathrm{V}}(V')G(V-V')\mathrm{d}V' \qquad (27)$$

where

$$G(V,V') = \frac{2\sqrt{2}}{nV'}\frac{\mathbf{K}\left(\frac{1-|V|/V'}{1+|V|/V'}\right)}{\sqrt{1+|V|/V'}} \qquad (28)$$

$\mathbf{K}$ is the full elliptic integral of the first kind [46]:

$$\mathbf{K}(k) = \int_0^{\pi/2}\frac{\mathrm{d}\varphi}{\sqrt{1-k^2\sin^2\varphi}}.$$

The main feature of the weighting function G consists of its logarithmic divergence at $V\to0$. This means that RCs with small effective (accounting for orientational factor γ given by equation (12)) activation volumes evidently tend to be more numerous. Physically this is due to the fact that the manifold of the sets of the angles θ and ψ mapping to zero orientational factor ($\theta = 0$ *or* $\theta = \pi/2$ *or* $\psi = \pm\pi/2$) is of dimension 1, while the manifold of the $\{\theta,\psi\}$ sets corresponding to the maximal value of γ ($\theta = \pi/4$ and $\psi = 0$) has zero dimension. The predominance of near-zero effective activation

volumes leads to important conclusions about the creep kinetics as will be shown in Section 7.

7. TEST EXAMPLE: "FLAT" ACTIVATION ENERGY SPECTRUM

A common hypothesis about the form of the activation energy spectrum is that this spectrum is quite uniform. To test the theory consider

$$\rho_E(E) = \rho_0 \tag{29}$$

where ρ_0 is some constant. This permits the application of equation (23) and calculation of creep kinetics for different spectra of activation volumes, $\rho_V(V)$. The results are represented by curves 1–5 in Fig. 3. It is seen that the observed creep kinetics, in fact, *does not depend on the form of* $\rho_V(V)$. The only important thing is whether the upper bound V_{up} of the spectrum $\rho_V(V)$ lies beyond the critical volume, $V_c = kT/\sigma$. If $V_{up} < V_c$ then the creep rate curve $\ln\dot{\varepsilon}$ ($\ln t$) has a "shelf" at short times $t \ll \tau$ caused by the lack of RCs with sufficiently low activation barriers. Indeed, the RCs with $E < kT \ln \nu\tau$ did not survive preannealing and the creep at short times t is provided by RCs with the lifetime

$$\tau_1 \cong \nu^{-1}\exp\left(\frac{(E - \sigma V_{up})}{kT}\right) > \tau\exp\left(\frac{-V_{up}}{V_c}\right) \tag{30}$$

which is large as compared with t. At this stage the number of such RCs decreases slowly in the scale of t and this is the reason the strain rate is almost constant. Note that the main contribution to the strain rate is from the RCs of near-zero effective activation volume, as was shown in preceding Section 6. When t reaches τ_1 these RCs start to anneal and the strain rate begins to slow down. In the opposite case, if there are RCs with $V > V_c$, then activation barriers for them become low under loading and the rate of RCs annealing, which determines also the creep strain rate, is large even at $t = 0$.

Since the exact form of the activation volume spectrum plays no role we can choose it as a single δ-peak: $\rho_V(V) = R\delta(V - V_0)$, where R and V_0 are constants. Then making use of the flat spectrum approximation (equation (29)) and taking into account equations (23), (24) and (28) we obtain

$$\dot{\varepsilon} = \varepsilon_0 \int_{-\infty}^{\infty} \frac{G(V, V_0)}{t + \tau e^{-\frac{\sigma V}{kT}}} dV \tag{31}$$

where

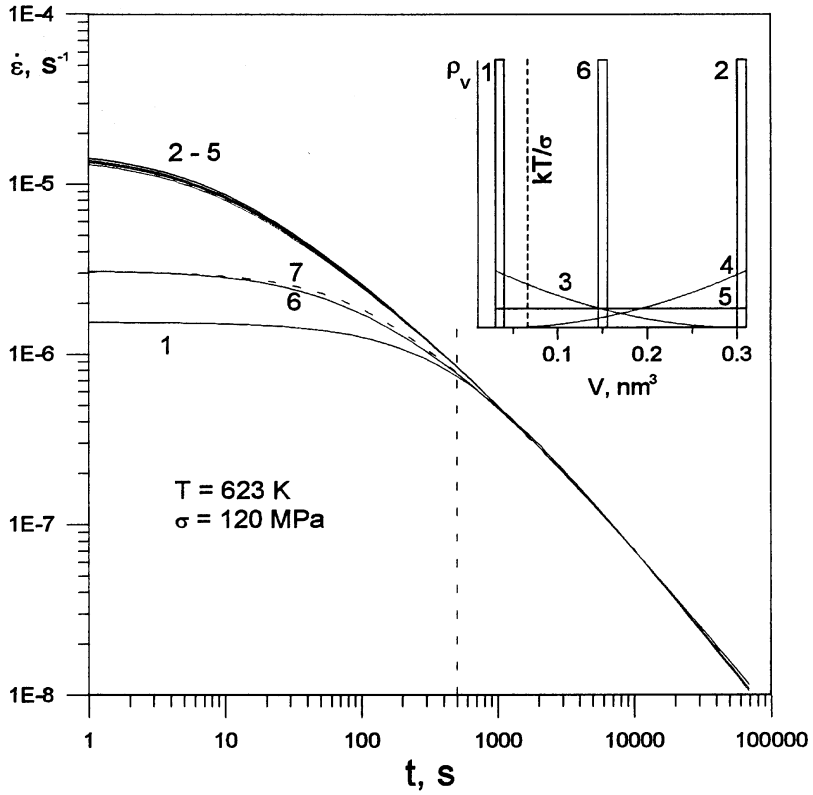

Fig. 3. Creep kinetics in the model of the flat activation energy spectrum. Curves 1–5 are calculated using equation (23) for different activation volume spectra shown in the inset by the corresponding numerals and $\tau = 500$ s (dashed vertical), $T = 623$ K, and $\sigma = 120$ MPa. Curves 6 and 7 are obtained according equation (31) and equation (32), correspondingly, with $V_0 = 0.15$ nm^3. All curves are normalized to merge at $t = 10\,000$ s.

$$\varepsilon_0 = \sigma k T N_0 \Omega C R \rho_0.$$

Previous versions of our theory [33–41, 44, 45] considered only two RC orientations: towards and against the applied shear stress. Nevertheless, these versions appear to be consistent with the present one. Indeed, according to the previous versions a refined expression for the creep strain rate due to irreversible relaxation under the flat spectrum approximation (29) has the form [37, 39, 40]

$$\dot{\varepsilon} = \frac{\sigma k T N_0 \Omega C \left[\mathrm{ch}\left(\frac{\sigma V_0}{\sqrt{3} k T} \right) + \frac{t}{\tau} \right]}{\tau \left[1 + 2 \frac{t}{\tau} \mathrm{ch}\left(\frac{\sigma V_0}{\sqrt{3} k T} \right) + \left(\frac{t}{\tau} \right)^2 \right]} \qquad (32)$$

where N_0 is the RC volume density per unit activation energy interval, the other quantities having the same meaning as previously indicated.

Curve 6 in Fig. 3 is calculated for $T = 623$ K and $\tau = 500$ s using equation (31) with $V_0 = 0.15\ \mathrm{nm}^3$ and curve 7 in this figure is obtained using equation (32) with the same parameters. It is seen that the curves are practically identical. This fact leads to the following inferences.

(i) The present version of the model is consistent with earlier ones, at least, under the assumptions that were made above.

(ii) Accounting for the orientational distribution of the RCs, in fact, does not lead to a noticeable change of calculated creep kinetics. Therefore, the latter may be written in the form of equation (32) which is considerably simpler compared to equation (31).

8. EXPERIMENTAL DETAILS

Metallic glass of nominal composition $Co_{57}Fe_5Ni_{10}Si_{11}B_{17}$ obtained by standard single roller quenching in the form of 15 μm thick ribbon was used for the investigation. X-ray diffraction and transmission electron microscopy were used to ensure the ribbon was entirely amorphous. Samples of 2–3 mm width were prepared from the ribbon. Creep measurements were carried out using a specially designed tensile apparatus with absolute resolution of about 30 nm (sample gauge length was equal to 50 mm). A sample, loaded by $\sigma \leq 5$ MPa, was heated at 5 K/min to the testing temperature T without overheating. The preannealing time τ was measured starting from $T - 5$ K. During the subsequent 200–300 s the sample temperature reached the required value T and was thereafter maintained within 0.5 K of this. After preannealing during time τ, the sample was loaded by a tensile stress of $\sigma = 195 \pm 20$ MPa and computer-controlled elongation measurements were started. The experiments were carried out in a vacuum of about 10^{-3} Pa at temperatures T of 573, 623 and 673 K and preannealing times τ of 500 and 3600 s.

9. EXPERIMENTAL RESULTS AND DISCUSSION

9.1. Creep stages

Figure 4 shows initial creep curves measured at $T = 573$ K after preannealing for 500 and 3600 s,

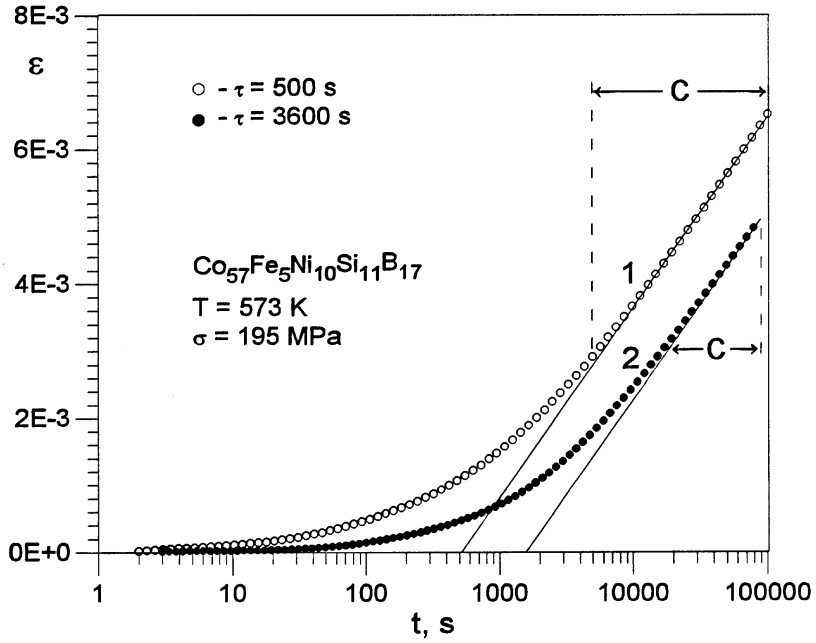

Fig. 4. Creep curves at $T = 573$ K and $\sigma = 195$ MPa after preannealing during $\tau = 500$ s (1) and 3600 s (2) in the logarithmic time-scale. Creep stage C is indicated.

plotted in the logarithmic time-scale. It is seen that at times considerably more than the preannealing time creep strain is proportional to the logarithm of time and ε–ln t dependences for various τ are parallel to each other. Analogous results were obtained for other testing temperatures. This means that the strain rate kinetics at long times can be described by the equation

$$\dot{\varepsilon} = \frac{A}{t} \tag{33}$$

and the quantity A is τ independent. The latter fact can be expressed such that under the condition $t \gg \tau$, the material loses memory of its thermal prehistory.

Meanwhile, these conclusions are in excellent agreement with the proposed theory in its simplest form. Indeed, under $t \gg \tau e^{-\sigma V/kT}$, equation (31) is equivalent to the experimental law of equation (33) with

$$A = \varepsilon_0 \int_{-\infty}^{\infty} G(V, V_0) \mathrm{d}V.$$

Let us analyze the experimental strain rate kinetics in more detail. Numerical differentiation of the initial creep curves results in large errors and, therefore, these curves were subjected to a preliminary special procedure of local smoothing [47]. Strain rate time dependences obtained after such a procedure for $\tau = 500$ s and all testing temperatures are shown in Fig. 5. These dependences are clearly nonmonotonic and this can be further documented by plotting the kinetics of the "strain rate time sensitivity coefficient" $m = \partial \ln \dot{\varepsilon} / \partial \ln t$ for various testing temperatures as shown in Fig. 6. Three creep stages, indicated as A, B and C can be distingnished in the $m(t)$ dependence.

The transition stage A is characterized by an increase of m and ends at the inflection point ($\partial m / \partial t = 0$). The duration of this stage depends on the preannealing time and amounts to 30–60 s for $\tau = 500$ s and 300–400 s for $\tau = 3600$ s. At the second transition stage, B, m decreases from its maximal value to $m \approx -1$. The duration of this stage can be estimated as 10τ. The third stage C is characterized by the constant value $m = -1$ within $\approx$10% accuracy. It is completely consistent with the proposed theory. Using equation (31) provides $m = -1$. Thus, the condition $t \gg \tau$ is a prerequisite to stage C.

By matching equation (33) with the experimental long-time strain rate data in the ln–ln plot it is possible to determine the unknown parameter ε_0 in equation (31). After that, treating V_0 as a fitting parameter, the model strain rate kinetics with the help of this equation can be calculated. The corresponding results for the testing temperature $T = 573$ K are shown as solid curves in Fig. 5. The numerals adjacent to these curves denote V_0 values used in the calculations and expressed in cubic nanometers. It can be concluded that with $V_0 = 0.09 \div 0.12\ \mathrm{nm}^3$, equation (31) fits creep stages B and C quite well. (Note that this volume is several times greater than the volume per atom, $\approx 0.03\ \mathrm{nm}^3$.) However, stage A cannot be described by this equation. An analogous situation is observed when fitting all other experimental creep curves.

Creep stage A is also clearly manifested on all time dependences of the Newtonian shear viscosity

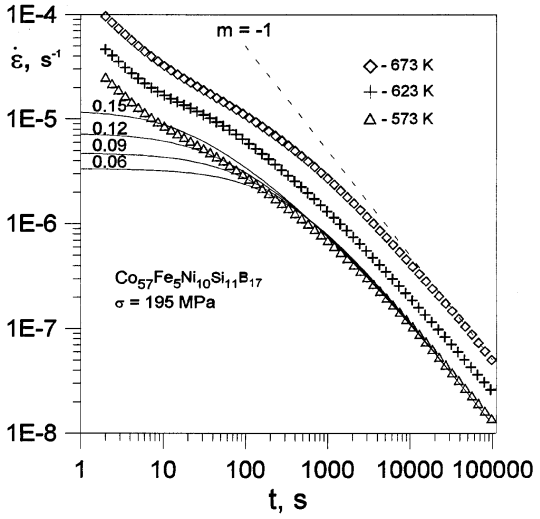

Fig. 5. Creep strain rate kinetics at various temperatures after preannealing during $\tau = 500$ s in the double-log coordinates. The dashed line is drawn with the slope $m = -1$. Solid curves are obtained for $T = 573$ K and $\sigma = 195$ MPa using equation (31) with V_0 values as indicated.

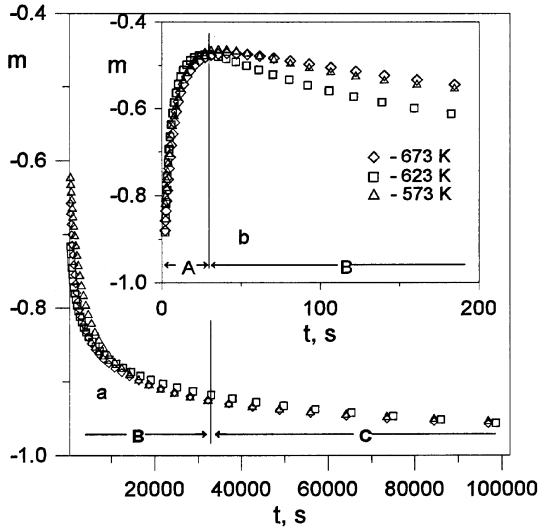

Fig. 6. Kinetics of the strain rate time sensitivity coefficient m at various temperatures and $\tau = 500$ s. The inset shows the initial part of the $m(t)$ dependence on an enlarged time-scale. Creep stages A, B and C are indicated.

$\eta = \sigma/3\dot{\varepsilon}$. A typical example is shown in Fig. 7 where the viscosity kinetics for $T = 573$ K and $\tau = 500$ s is presented. It is seen that the beginning of creep is characterized by a nonlinear viscosity increase and usual linear behavior is observed after that. However, model calculations (solid line) reproduce only the latter. Therefore, it is concluded that the developed theory gives a good approximation of creep stages B and C and fails to describe stage A. Note that both stages, B and C, result in linear viscosity growth with time whereas pure logarithmic creep corresponds only with stage C.

The experimental data for a Ni-based MG is completely analogous to those described above [39, 40].

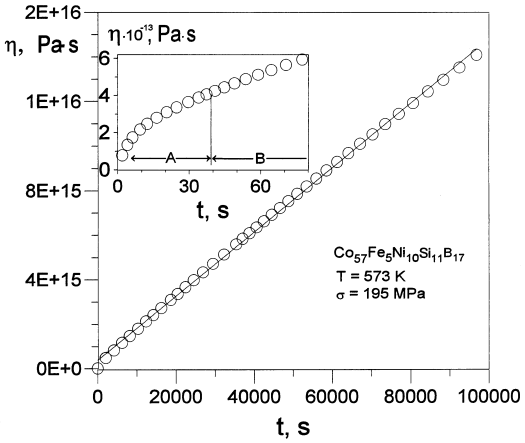

Fig. 7. Kinetics of the Newtonian viscosity at $T = 573$ K after preannealing during $\tau = 500$ s. The inset shows the initial part of the $\eta(t)$ dependence on an enlarged time-scale. Creep stage A and the beginning of stage B are indicated. The solid line is drawn using equation $\eta(t) = \sigma/3\dot{\varepsilon}(t)$ with $\dot{\varepsilon}(t)$ determined from equation (31).

9.2. On the nature of the stage A

Let the process responsible for creep stage A be called A-relaxation and the corresponding strain rate be denoted as $\dot{\varepsilon}_A$. The A-relaxation cannot be explained by some feature of the initial relaxation spectrum $w(E,V)$ since it combines, as compared with stage C, high annealing rate with relatively low creep strain rate. Such a scenario could be caused by a small number of RCs with low activation barriers. Low barriers could be due either to low activation energy (but all such RCs must relax during preannealing), or to large activation volume and advantageous orientation, but if there are RCs with large activation volumes then the situation discussed in Section 7 applies. This situation is unsuitable for the A-relaxation.

We suppose the A-relaxation is a manifestation of the *reversible* structural relaxation. A possibility of such a relaxation in MG is confirmed by the known effect of partial strain recovery after unloading [48, 49]. From the phenomenological viewpoint, the reversible relaxation is provided by the RCs, which have an effective potential relief with two neighboring equivalent wells separated by a potential barrier E. The number of such reversible RCs (RRCs) is small because potential wells may be considered as equivalent only if their depths differ by no more than kT while the typical difference must be of the order of the energy spectrum range E_{up} for MG measured in electronvolts. Provided a flat distribution of depth differences exists, the following estimate for the number N_r of RRCs can be obtained:

$$\frac{N_r}{N_0} = \frac{kT}{E_{up}}. \tag{34}$$

There is no resulting flow between the equivalent wells without loading. In other words, RRCs are not annealed before loading. An accurate analysis of RRC-related creep kinetics will be published elsewhere but the main effect is quite clear: the preannealing time τ in formulae of the type given by equation (31) approaches zero and deformation becomes multiplied by the small factor N_r/N_0 given by equation (34). Then the reversible component of creep strain rate can be estimated as

$$\dot{\varepsilon}_A \sim \frac{kT}{E_{up}} \frac{\varepsilon_0}{t} \tag{35}$$

giving the strain rate time sensitivity coefficient $m = -1$. (Note that the same m value for the A-relaxation was obtained in Ref. [40] while using considerably different reasoning.) The inset in Fig. 6 clearly demonstrates that m just tends to this value at the beginning of stage A. So, the contribution from reversible relaxation processes at short creep times may be comparable with that determined by the irreversible relaxation.

It was shown above that the proposed model quantitatively explains all details (except A-relaxation) of the experiment which was especially carried out in order to test the theory. The only thing that has not been verified experimentally is whether this theory is able to describe correctly the transition from Newtonian to nonlinear flow with increasing applied stress. The corresponding experiment has to be performed. However, the predicted results of this experiment are expected because both equation (31) and equation (32) imply the possibility of this transition.

10. CONCLUSIONS

An extended version of the theory of irreversible structural relaxation of metallic glasses in an external stress field has been presented. The theory implies structural relaxation to be a result of two-stage elementary shear rearrangements in particular regions of the structure—relaxation centres (RCs)—and accounts for distributions of their activation

energies, activation volumes and orientation with respect to the applied stress.

Precision creep investigations of a Co-based metallic glass have shown that three stages in strain rate time dependences can be distinguished. These stages, named A, B and C, differ in the kinetics of strain rate time sensitivity coefficient $m = \partial \ln \dot{\varepsilon} / \partial \ln t$.

It has been recognized that the stages B and C can be completely described by the proposed theory in its simplest form: absence of coupling of activation parameters and "flat" activation energy spectra. It has been shown that the orientational distribution of RCs and distribution of their activation volumes are insignificant for creep kinetics.

It is argued that the initial creep stage A, which covers the time interval from several tens to several hundreds of seconds, depending on the preannealing time, is determined by reversible rearrangements in the RCs with symmetrical two-well potential. The contribution of this stage to the total creep strain can be comparable with that of stages B and C induced by irreversible atomic rearrangements.

Acknowledgements—The help of N. P. Kobelev (RAS Institute of Solid State Physics, Chernogolovka, Moscow district) is greatly acknowledged.

REFERENCES

1. Taub, A. I. and Spaepen, F., *Scripta metall.*, 1979, **13**, 195.
2. Spaepen, F., *Acta metall.*, 1977, **25**, 407.
3. Argon, A. S., *Acta metall.*, 1979, **27**, 47.
4. Taub, A. I. and Spaepen, F., *Acta metall.*, 1980, **28**, 1781.
5. Tsao, S. S. and Spaepen, F., *Proc. Int. Couf. on Rapid Quench. Metals Sendai*, 1981, **1**, 463.
6. Tsao, S. S. and Spaepen, F., *Acta metall.*, 1985, **33**, 891.
7. Volkert, C. A. and Spaepen, F., *Acta metall.*, 1989, **37**, 1355.
8. van den Beukel, A. and Radelaar, S., *Acta metall.*, 1983, **31**, 419.
9. van den Beukel, A., van der Zwaag, S. and Mulder, A. L., *Acta metall.*, 1984, **32**, 1895.
10. van den Beukel, A. and Huizer, E., *Scripta metall.*, 1985, **19**, 1327.
11. van den Beukel, A., Huizer, E. and van der Zwaag, S., *Acta metall.*, 1986, **34**, 483.
12. van den Beukel, A., *Acta metaIl.*, 1991, **39**, 2709.
13. van den Beukel, A., *Physica status solidi (a)*, 1991, **128**, 285.
14. van den Beukel, A., *Physica status solidi (a)*, 1992, **129**, 49.
15. van den Beukel, A. and Sietsma, J., *Mater. Sci. Engng*, 1994, **A179/A180**, 86.
16. van den Beukel, A., *Acta metall. mater.*, 1994, **42**, 1273.
17. Primak, W., *Phys. Rev.*, 1955, **100**, 1677.
18. Argon, A. S., *J. appl. Phys.*, 1968, **39**, 4080.
19. Argon, A. S. and Kuo, H. Y., *J. Non-Cryst. Sol.*, 1980, **37**, 241.
20. Gibbs, M. R. J., Evetts, J. E. and Leake, J. A., *J. Mater. Sci.*, 1983, **18**, 278.
21. Gibbs, M. R. J. and Sinning, H.-R., *J. Mater. Sci.*, 1985, **20**, 2517.
22. Sinning, H.-R., Leonardsson, L. and Cahn, R.W., *Int. J. Rapid Solidif.*, 1984–85, **1**, 175.
23. Hernando, A., Nielsen, O. V. and Madurga, V., *J. mater. Sci.*, 1985, **20**, 2093.
24. Friedrichs, H. and Neuhauzer, H., *J. Phys: Condens. Matter*, 1989, **1**, 8305.
25. Dzuba, G. A., Zolotukhin, I. V., Kosilov, A. T. and Khonik, V. A., *Fizika tverd. Tela*, 1991, **33**, 3393 (Translated in: *Sov. Phys. Solid State* **33**, 1913 (1991).).
26. Khonik, V. A. and Kosilov, A. T., *J. Non-Cryst. Sol.*, 1994, **170**, 270.
27. Kursumovic, A., Scott, M. G. and Cahn, R. W., *Scripta metall. mater.*, 1990, **24**, 1307.
28. Csach, K., Ocelik, V., Miskuf, J. and Bengus, V. Z., *IEEE Trans. Magn.*, 1994, **30**, 496.
29. Kasardova, A., Ocelik, V., Csach, K. and Miskuf, J., *Phil. Mag. Lett.*, 1995, **71**, 257.
30. Knuyt, G., Stals, L. M., de Schepper, L. and de Ceuninck, W., *Mater. Sci. Engng*, 1991, **A133**, 340.
31. Taub, A. I., *Acta metall.*, 1980, **28**, 633.
32. Taub, A. I. and Luborsky, F. E., *Acta metall.*, 1981, **29**, 1939.
33. Kosilov, A. T. and Khonik, V. A., *Izvestiya RAN, Seriya Fizicheskaya*, 1993, **57**, 192 (Translated in: *Bull. Russ. Acad. Sci. (USA)* **57**, 2033 (1993).).
34. Khonik, V. A., Kosilov, A. T. and Mikhailov, V. A., *J. Non-Cryst. Sol.*, 1995, **192-193**, 420.
35. Belyavsky, V. I., Bobrov, O. P., Kosilov, A. T. and Khonik, V. A., *Fizika tverd. Teza*, 1996, **38**, 28 (Translated in: *Phys. Solid. State (USA)* **38**, 16 (1996).).
36. Bobrov, O. P., Kosilov, A. T. and Khonik, V. A., *Fizika metall. Metalloved.*, 1996, **81**, 123 (Translated in: *Phys. Met. Metallogr.* **81**, 318 (1996).).
37. Bobrov, O. P., Kosilov, A. T., Mikhailov, V. A. and Khonik, V. A., *Izvestiya RAN, Seriya Fizicheskaya*, 1996, **60**, 124.
38. Bobrov, O. P., Kosilov, A. T. and Khonik, V. A., *Fizika tverd. Teza*, 1996, **38**, 1086 (Translated in: *Phys. Solid State (USA)* **38**, 601 (1996).
39. Kosilov, A. T., Mikhailov, V. A., Khonik, V. A. and Csach, K., *Fizika metall. Metalloved.*, 1996, **82**, 172 (Translated in: *Phys. Met. Metallogr.* **82**, 549 (1996).
40. Csach, K., Khonik, V. A., Kosilov, A. T., Mikhailov, V. A., *Proc. 9th Int. Conf on Rapidly Quenched and Metastable Materials* (Supplement), ed. P. Duhaj, P. Mrafko and P. Svec. Elsevier, Amsterdam, 1997, p.357.
41. Bobrov, O. P., Kosilov, A. T. and Khonik, V. A., *Fizika tverd. Teza*, 1996, **38**, 3059 (Translated in: *Phys. Solid State (USA)* **38**, 1673 (1996).
42. Belyavsky, V. I., Bobrov, O. P., Khonik, V. A. and Kosilov, A. T., *J. de Physique IV*, 1996, **6**, C8–715.
43. Khonik, V. A., Mikhailov, V. A. and Vinogradov, A. Yu., *Scripta mater.*, 1997, **37**, 377.
44. Khonik, V. A., Mikhailov, V. A. and Safonov, I. A., *Scripta mater.*, 1997, **37**, 921.
45. Bobrov, O. P., Khonik, V. A. and Zhelezny, V. S., *J. Non-Cryst. Sol.*, 1997, **223**, 241.
46. Abramowitz, M. and Stegun, I. A., ed., *Handbook of Mathematical Functions.* National Bureau of Standards, Washington, DC, 1964.
47. Turchak, L. I., *Fundamentals of Numerical Methods.* Nauka, Moscow, 1987, p.74 (in Russian).
48. Berry, B. S., in *Metallic Glasses*, ed. J. J. Gilman and H. J. Leamy. American Society of Metals, Cleveland, OH, 1978, p. 161.
49. Khonik, V. A., Kosilov, A. T., Kuzmitschev, V. A. and Dzuba, G. A., *Acta metall. mater.*, 1992, **40**, 1387.